Appl. Phys. B 75, 695–701 (2002)
DOI: 10.1007/s00340-002-1010-9

Applied Physics B
Lasers and Optics

D.K. GRAMOTNEV✉
D.F.P. PILE

Extremely asymmetrical scattering in gratings with weak dissipation: some physical analogies

Applied Optics Program, Centre for Medical, Health and Environmental Physics, School of Physical and Chemical Sciences, Queensland University of Technology, GPO Box 2434, Brisbane 4001, Australia

Received: 19 February 2002/Revised version: 28 June 2002
Published online: 22 November 2002 •

ABSTRACT A detailed analysis of new effects related to extremely asymmetrical scattering (EAS) of bulk and guided weakly dissipating electromagnetic waves in oblique periodic gratings is presented. A very important role of the previously determined critical grating width is demonstrated for EAS in dissipative gratings. Incident and scattered wave amplitudes inside and outside the grating are analysed as functions of dissipation coefficient, grating width, grating amplitude, etc. Strong differences in the patterns of scattering in gratings that are narrower and wider than the critical width are demonstrated and discussed. Deep analogies between EAS and other resonant optical effects, such as attenuated total reflection, Fabry–Pérot interferometry, etc. are revealed and discussed. A physical interpretation of the obtained results is presented.

PACS 42.25.Fx; 42.79.Dj; 42.40.Eq

1 Introduction

Extremely asymmetrical scattering (EAS) is a type of Bragg scattering in wide strip-like periodic gratings with the scattered wave propagating parallel to the grating boundaries [1–10]. EAS has been shown to be radically different from the conventional scattering in transmitting and reflecting periodic gratings. The main unique features of EAS include a strong resonant increase of the scattered wave amplitudes inside and outside the grating (the smaller the grating amplitude, the larger the amplitude of the scattered wave) [1–8, 10], a highly unusual frequency response of EAS with an additional strong resonance in the side-lobe structure of the reflected signal [11], an additional strong resonance with respect to the angle of scattering when the scattered wave propagates at a grazing angle with respect to the grating boundaries (grazing-angle scattering) [7], an unusually high sensitivity of EAS to small variations of mean structural parameters across the grating [10], two simultaneous resonances in non-uniform gratings with varying phase [5, 6], etc.

It has also been demonstrated that the main physical reason for all these physical effects is the diffractional divergence of the scattered wave inside and outside the grating (similar to divergence of a laser beam of finite aperture) [1–8, 10]. The necessity of taking the divergence into account can easily be seen from the following consideration. The scattered wave results from scattering of the incident wave inside the grating, and propagates parallel to the grating (the geometry of EAS). Therefore, it must be represented by a beam located within the grating and having the aperture that is equal to the grating width. It is obvious that such a beam will diverge outside the grating due to diffractional divergence. Thus, on the one hand, the scattered wave amplitude must increase due to scattering of the incident wave in the grating, and, on the other hand, it must decrease due to diffractional divergence. In the absence of dissipation, the competition of these two opposing mechanisms results in a steady-state pattern of EAS, where the contributions to the scattered wave amplitude due to divergence and scattering are cancelled [1–3].

One of the strongest confirmations of the essential role of diffractional divergence in the geometry of EAS comes from the existence of a critical grating width [5–7, 10]. The pattern of EAS appears to be substantially different in gratings that are narrower and wider than the critical width (narrow and wide gratings) [5–7, 10]. Physically, half of the critical width is equal to the distance within which the scattered wave can be spread across the grating by means of diffractional divergence, before being re-scattered by the grating [5, 6].

On the basis of the presented physical interpretation of EAS, a new approximate method of analysis of this type of scattering has been developed [1–3, 7, 11]. It is based on the separate consideration of scattering and diffractional divergence, and subsequent comparison of their contributions [1–3, 7, 11]. The main advantages of this method include a new insight into the physical processes in gratings [1–7, 10], direct applicability for the analysis of scattering of all types of waves (including surface and guided optical and acoustic modes) in different types of periodic gratings [1–4, 6, 10], and simple analytical solutions even for complex multi-layer structures [1]. The comparison with the rigorous method of analysis [9] has demonstrated a high degree of accuracy of the approximate method for the most interesting cases of EAS with a strong resonant increase of the scattered wave amplitude [9, 10]. Applicability conditions for the approximate method have been derived and discussed [7, 9].

✉ Fax: +61-7/3864-9079, E-mail: d.gramotnev@qut.edu.au

Recently, the developed approximate method has been extended to the case of weakly dissipating waves in periodic gratings [8]. The corresponding coupled wave equations have been derived [8]. In particular, it has been shown that weak dissipation can substantially affect the pattern of scattering in the geometry of EAS, resulting in a noticeable reduction of the scattered wave amplitudes, especially near the rear boundary of a wide grating [8]. However, no detailed analysis of EAS in wide and narrow gratings with weak dissipation has been carried out. The role of the critical width has not been investigated for EAS of weakly dissipating waves. In addition, detailed analysis of EAS of dissipating waves can be expected to reveal interesting analogies between EAS and other resonant optical effects, such as attenuated total reflection (ATR) [12–14], resonant interference in a Fabry–Pérot interferometer [15], resonant transparency of opaque metal films [16, 17], resonant rotation of a mirror-reflected wave [18], etc.

Therefore, the aim of this paper is to present a detailed investigation of EAS of bulk and guided optical waves in periodic dissipative gratings. In particular, amplitudes of the incident and scattered waves inside and outside the grating will be analysed as functions of the dissipation coefficient (i.e. the imaginary part of the wave number). The role of the critical grating width for EAS of weakly dissipating waves will be investigated. Deep analogies between EAS and other resonant effects will be revealed and discussed.

2 Structure and method of analysis

Let a plane bulk TE electromagnetic wave with a wavevector $\boldsymbol{k}_0$ and an amplitude E_{00} be incident at an angle θ_0 (measured from the x axis counter-clockwise (Fig. 1)) onto a holographic grating represented by small sinusoidal variations of the dielectric permittivity within a region of thickness L (Fig. 1):

$$\varepsilon_\mathrm{s} = \begin{cases} \varepsilon + \left[\varepsilon_1 \mathrm{e}^{\mathrm{i}Q_x x + \mathrm{i}Q_y y} + \varepsilon_1^* \mathrm{e}^{-\mathrm{i}Q_x x - \mathrm{i}Q_y y}\right] & \text{if } 0 < x < L, \\ \varepsilon & \text{otherwise,} \end{cases} \quad (1)$$

where $\varepsilon = e_1 + \mathrm{i}e_2$ is the complex mean dielectric permittivity that is the same throughout the structure, ε_1 is the grating amplitude, Q_x and Q_y are the x and y components of the reciprocal lattice vector $\boldsymbol{Q}$, $Q = 2\pi/\Lambda$, Λ is the grating period, the coordinate system (x, y) is presented in Fig. 1, and the x_0 axis is parallel to the vector $\boldsymbol{Q}$. The extension of the grating along the y and z axes is infinite.

It is also assumed that the dissipation of electromagnetic waves is weak:

$$e_2 \ll e_1 > 0 \quad (2)$$

and the grating amplitude is small compared to the real part of the mean permittivity in the structure:

$$\left|\frac{\varepsilon_1}{\varepsilon}\right| \ll 1 . \quad (3)$$

If conditions (2) and (3) are satisfied, then periodic variations of the dissipation in the grating are of the second order of the ratio $|\varepsilon_1/\varepsilon|$ and can be neglected. In other words, the term in the square brackets in (1) is real. Thus the dissipation should be taken into account by means of the constant small imaginary part e_2 of the mean permittivity ε inside and outside the grating.

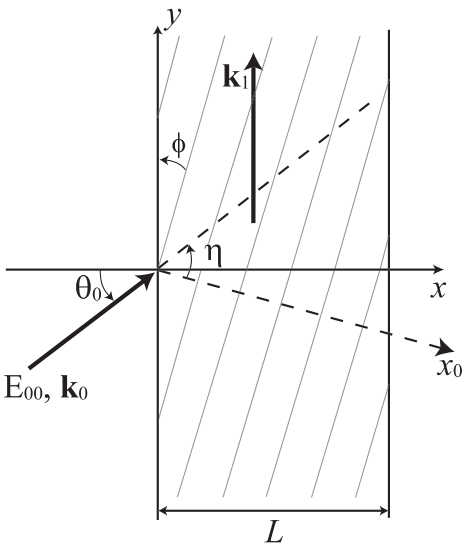

FIGURE 1 Structure for EAS in a uniform grating with dissipation

We assume that the Bragg condition is satisfied precisely:

$$\boldsymbol{k}_1 - \boldsymbol{k}_0 = -\boldsymbol{Q} , \quad (4)$$

where $\boldsymbol{k}_0$ and $\boldsymbol{k}_1$ are the real parts of the wave vectors of the incident and scattered waves, and $\boldsymbol{k}_1$ is parallel to the grating boundaries (Fig. 1).

In [8], using the approximate method based on the allowance for the diffractional divergence, we obtained the coupled wave equations for the considered problem:

$$\frac{\mathrm{d}^2 E_1(x)}{\mathrm{d}x^2} + 2\mathrm{i}\alpha_1 k_1 E_1(x) + K_0 E_0(x) = 0 , \quad (5)$$

$$\frac{\mathrm{d}E_0(x)}{\mathrm{d}x} + \frac{\alpha_0 E_0(x)}{\cos(\theta_0)} - \mathrm{i}K_1 E_1(x) = 0 , \quad (6)$$

where $K_0 = -2k_1 \Gamma_0 \sin(\eta - \theta_0)$, $K_1 = \Gamma_1 \cos(\eta)/\cos(\theta_0)$, η is the angle measured from the x_0 axis to the wave vector of the incident wave counter-clockwise, α_0 and α_1 are the imaginary parts of the wave numbers of the incident and scattered waves, respectively, $E_0(x)$ and $E_1(x)$ are the slowly varying amplitudes of the incident and scattered waves inside the grating, and Γ_0 and Γ_1 are the coupling coefficients determined in the conventional theories of Bragg scattering in a grating with the fringes parallel to the grating boundaries [19–27]. For example, for bulk TE electromagnetic waves in a non-dissipative grating described by (1) in an isotropic medium, we have: $\alpha_1 = \alpha_0$, $k_1 = k_0$, and the explicit equations for the coupling coefficients can be written as [21]:

$$\Gamma_0 = -\Gamma_1^* = -\frac{\varepsilon_1^* \omega^2}{2c^2 k_0 \cos(\eta)} , \quad (7)$$

where c is the speed of light in vacuum and ω is the frequency of the wave. Note that unlike (7) (which is correct only for bulk TE waves in holographic gratings), (5) and (6) are directly applicable for all types of waves, including bulk,

guided, and surface electromagnetic and acoustic waves in various types of periodic gratings with weak dissipation. For example, for the extension of this theory to optical modes guided by a slab with a corrugated boundary see Sect. 4.

3 Analysis

It has been demonstrated that there exists a critical width L_c [6, 7] that determines narrow and wide gratings with distinctly different patterns of scattering [6–8]. Physically, half of the critical width is equal to the distance within which the scattered wave can be spread across the grating by means of the diffractional divergence, before being re-scattered by the grating [6, 7]. Therefore, if the grating width $L < L_c$, then the diffractional divergence is highly effective in smoothing out variations of the scattered wave amplitude across the grating, and this amplitude can only weakly depend on distance from the front grating boundary [6–8, 10]. On the contrary, if $L > L_c$ (wide gratings), the scattered wave amplitude in the grating strongly depends on the x coordinate (Fig. 1) [6–8, 10].

The critical width for a uniform grating without dissipation is given by [5, 6]:

$$L_c \approx 4\left[\frac{1}{\mathrm{e}k_1}\left|\frac{E_1|_{x=0}}{\Gamma_0 E_{00}\sin(\eta-\theta_0)}\right|\right]^{1/2}, \qquad (8)$$

where $\mathrm{e} \approx 2.718$ and $E_1|_{x=0}$ is the amplitude of the scattered wave at the front boundary in a wide grating (i.e. in the case of $L > L_c$) without dissipation. Therefore, to determine L_c, we need to take a grating of a particular width L, calculate L_c using (8), and then, if the resultant value of L_c is less than L, the critical width is determined correctly. If L_c appears to be larger than L, then we have to recalculate L_c using a larger value for L until we get $L_c < L$, and this will be the right value for L_c [5, 6]. Though (8) has been derived for gratings without dissipation, it will be demonstrated below that the critical grating width (8) also plays a very important role for EAS of weakly dissipating waves.

Figures 2 and 3 present typical dependences of the relative amplitudes of the scattered (Fig. 2) and incident (Fig. 3) bulk TE electromagnetic waves on the x coordinate inside and outside the gratings of different widths L and for different imaginary parts of the mean permittivity. The other structural parameters are the same for all the curves in Figs. 2 and 3: $e_1 = 5$, $\varepsilon = 5 \times 10^{-3}$, and the wavelength in vacuum $\lambda = 1\ \mu$m; the orientation and period of the grating are determined by the Bragg condition: $\Lambda \approx 0.584\ \mu$m and $\phi = 22.5°$.

The main feature that can be seen from Figs. 2 and 3 is that (as expected) EAS is very sensitive to small dissipation of the waves. For example, increasing the imaginary part e_2 of the mean permittivity from 0 to 5×10^{-6} results in noticeable variations in the pattern of steady-state EAS – compare curves 1 with curves 2 in Figs. 2 and 3. Typical scattered wave amplitudes inside the gratings in this case are reduced by up to $\sim 10\%$–20% compared to EAS without dissipation (Fig. 2). Outside the gratings, the scattered wave amplitude appears to decay exponentially with increasing distance from the grating boundaries (Fig. 2).

It can be seen that in narrow gratings (e.g. for $L = 10\ \mu\mathrm{m} < L_c \approx 27.4\ \mu$m) [5, 6] the x-dependence of the scattered wave inside and outside the grating is almost symmetric with respect to the middle of the grating (Fig. 2a). If the grating width is increased to one critical width: $L \approx 27.4\ \mu$m (Fig. 2b), then weak dissipation makes the x-dependences of the scattered wave amplitudes significantly non-symmetric with respect to the middle of the grating. This effect becomes even more obvious if the grating width is increased further – see Fig. 2c.

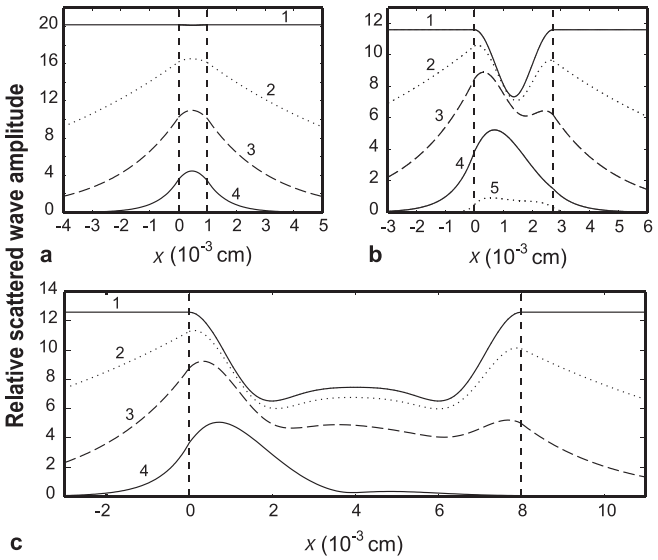

FIGURE 2 The dependences of the relative scattered wave amplitude $|E_1(x)/E_{00}|$ on distance from the front boundary for weakly dissipating bulk TE electromagnetic waves for different values of the imaginary part of the mean permittivity: **a** $L = 10\ \mu$m, (1) $e_2 = 0$, (2) $e_2 = 5 \times 10^{-6}$, (3) $e_2 = 5 \times 10^{-5}$, (4) $e_2 = 5 \times 10^{-4}$. **b** $L = L_c \approx 27.4\ \mu$m, (1) $e_2 = 0$, (2) $e_2 = 5 \times 10^{-6}$, (3) $e_2 = 5 \times 10^{-5}$, (4) $e_2 = 5 \times 10^{-4}$, (5) $e_2 = 5 \times 10^{-3}$. **c** Same as for (a) except that $L = 80\ \mu$m. The other structural parameters: $\varepsilon = 5 + \mathrm{i}e_2$, $|\varepsilon_1| = 5 \times 10^{-3}$, $\theta_0 = \pi/4$, $\eta = 3\pi/8$, and the wavelength in vacuum $\lambda = 1\ \mu$m; the grating period $\Lambda \approx 0.584\ \mu$m and the slanting angle $\phi = 22.5°$ are determined by the Bragg condition. *Vertical dashed lines* represent the grating boundaries

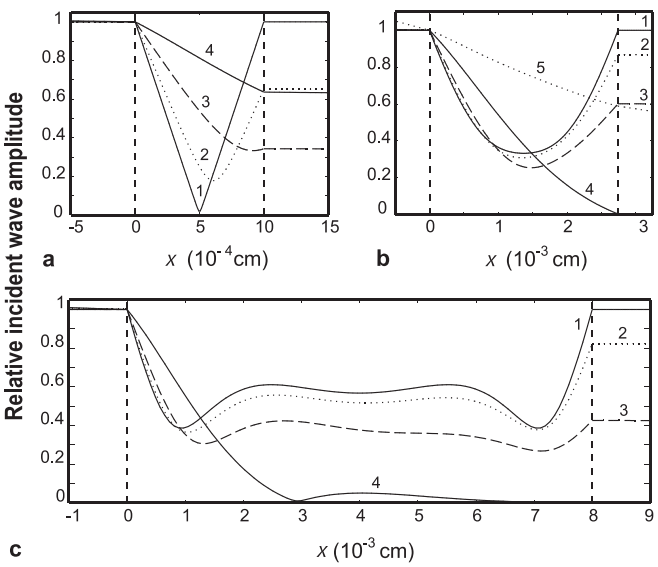

FIGURE 3 The dependences of the relative incident wave amplitude $|E_0(x)/E_{00}|$ on distance from the front boundary for weakly dissipating bulk TE electromagnetic waves in exactly the same structures as for Fig. 2a–c: **a** $L = 10\ \mu$m, (1) $e_2 = 0$, (2) $e_2 = 5 \times 10^{-6}$, (3) $e_2 = 5 \times 10^{-5}$, (4) $e_2 = 5 \times 10^{-4}$. **b** $L = L_c \approx 27.4\ \mu$m, (1) $e_2 = 0$, (2) $e_2 = 5 \times 10^{-6}$, (3) $e_2 = 5 \times 10^{-5}$, (4) $e_2 = 5 \times 10^{-4}$, (5) $e_2 = 5 \times 10^{-3}$. **c** Same as for (**a**) except that $L = 80\ \mu$m

This is expected since the steady-state amplitudes are achieved first near the front boundary, and then start spreading into a wide grating. Thus the relaxation time at the rear boundary appears to be significantly larger (see also [3, 4]), and the scattered wave amplitudes near this boundary are more sensitive to weak dissipation.

Note also that in wide gratings with $L > L_c$ the steady-state scattered wave amplitudes at the front boundary at a given dissipation (i.e. at a given value of e_2) hardly depend on grating width at all. This is because the diffractional divergence is not able to spread the scattered waves from the front or rear boundaries across a wide grating, because of re-scattering and dissipation of these waves in the grating. Therefore the scattered wave at the front boundary 'does not feel' what happens at the rear boundary for all values of e_2. At the same time, the amplitudes of the scattered wave at the rear boundary strongly depend on L – compare Fig. 2a–c. As mentioned above, this is mainly related to increasing relaxation time at the rear boundary with increasing L.

Typical coordinate dependences of the relative incident wave amplitude inside the gratings with weak dissipation are presented in Fig. 3a–c for the same structures as Fig. 2a–c. As can be seen from Fig. 3a–c, the x-dependences of the incident wave amplitudes are also strongly dependent on grating width.

For narrow gratings (with $L < L_c$), the minimal value of the incident wave amplitude inside the grating increases with increasing weak dissipation – see curves 1–4 in Fig. 3a. In addition, the position of this minimum moves from the middle of the grating (at $e_2 = 0$) to its rear boundary (at $e_2 \geq 5 \times 10^{-5}$) – Fig. 3a. Small variations of e_2 (e.g. from 0 to 5×10^{-6}) result in substantial variations (up to 30%) in the incident wave amplitude inside the grating (see Fig. Fig. 3a). Note that if we decrease the grating width further, the dependences in Fig. 3a will hardly change, except for the range of x on the horizontal axis (which corresponds to the grating width) and actual values of e_2 corresponding to these dependences. Therefore, Fig. 3a is typical for EAS in narrow gratings with $L < L_c$.

If the grating width $L = L_c \approx 27.4\,\mu\text{m}$ (Fig. 3b), then the dependences of the incident wave amplitude change significantly. For example, minimal values of this amplitude inside the grating are no longer increasing functions of e_2. On the contrary, these minimal values noticeably decrease with increasing e_2 from zero (see curves 1–4 in Fig. 3b). Further increase of e_2 results in increasing minimal values of $E_0(x)$ in the grating (see curve 5 in Fig. 3b). Typical shapes of the dependences presented in Fig. 3b are also noticeably different from those in Fig. 3a. Similar statements can be made regarding even wider gratings (Fig. 3c). In addition, it can be said that as a result of weak dissipation, the x-dependences of the incident wave amplitude become strongly non-symmetric with respect to the middle of the grating for all values of L (compare curves 1 with other curves in Fig. 3a–c).

Figure 3a–c demonstrate an interesting behaviour of the amplitude $E_{01} \equiv E_0\,|_{x=L}$ of the incident wave at the rear boundary (i.e. the wave transmitted through the grating). Initially, this amplitude decreases with increasing e_2, reaches a minimum (at $e_2 \approx 5 \times 10^{-5}$ in Fig. 3a and $e_2 \approx 5 \times 10^{-4}$ in Fig. 3b), and then increases back to about E_{00} – the amplitude of the incident wave at the front boundary. Further increasing the imaginary part of the mean permittivity results in decreasing amplitude of the transmitted wave E_{01}, and for large dissipation E_{01} it monotonically tends to zero. This is the general trend for all grating widths (Fig. 3a–c). More explicitly, it is illustrated by Fig. 4, where relative transmitted wave amplitudes $|E_{01}/E_{00}|$ are presented as functions of the imaginary part of the mean permittivity e_2 for different grating widths. All the curves in this figure tend to 1 as $e_2 \to 0$, which corresponds to EAS without dissipation. This is the consequence of energy conservation [3–7]. As expected, for large e_2, all the curves tend to zero. This is related to the overall strong dissipation in the structure, so that the waves cannot propagate through the grating without substantial decay.

The minima within the interval of e_2 from $\sim 10^{-6}$ to $\sim 10^{-4}$ cannot be explained just by the dissipation of the incident wave in the grating. Indeed, typical distances through which this wave can propagate in media with such values of e_2 vary from ≈ 4 cm to ≈ 0.4 cm, and this is much larger than the grating width. These minima are explained by the interaction of the incident and scattered waves inside the grating, and dissipation of the scattered wave.

Indeed, the scattered wave re-scatters in the grating. The re-scattered wave propagates in the direction of the incident wave, and is approximately in antiphase with the incident wave [6]. As a result, for narrow gratings in the absence of dissipation, the amplitude of the incident wave decreases almost linearly from E_{00} at the front boundary to about zero in the middle of the grating (see curve 1 in Fig. 3a), where the incident wave is cancelled by the re-scattered wave. That is, in the first half of the grating (i.e. at $0 < x < L/2$) the energy flows from the incident wave into the scattered wave. In the second half of the grating (i.e. at $L/2 < x < L$) the amplitude of the re-scattered wave becomes larger than E_{00}. As a result, the overall magnitude of the incident wave amplitude increases from about 0 (in the middle of the grating) back to $|E_{00}|$ at the

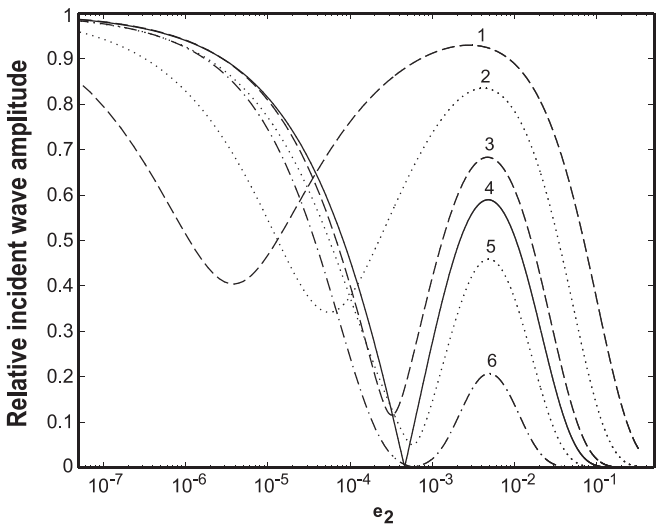

FIGURE 4 The dependences of the relative transmitted wave amplitude $|E_{01}/E_{00}|$ at the rear grating boundary, $x = L$, on the imaginary part e_2 of the mean permittivity ε for different grating widths: (1) $L = 5\,\mu$m, (2) $L = 10\,\mu$m, (3) $L = 20\,\mu$m, (4) $L = L_c \approx 27.4\,\mu$m, (5) $L = 40\,\mu$m, (6) $L = 80\,\mu$m. The other structural parameters: $\varepsilon = 5 + \mathrm{i}e_2$, $|\varepsilon_1| = 5 \times 10^{-3}$, $\theta_0 = \pi/4$, $\eta = 3\pi/8$, $\lambda = 1\,\mu$m

rear boundary (curve 1 in Fig. 3a). Thus in the second half of the grating the energy flows back from the scattered wave into the incident wave [6].

If e_2 is non-zero but sufficiently small, and the grating width is not too large (so that $\alpha_0 L/\cos(\theta_0) \ll 1$), then the dissipation of the incident wave, as it propagates across the grating, can be neglected: $E_{00}\exp\{-\alpha_0 L/\cos(\theta_0)\} \approx E_{00}$. However, dissipation of the scattered wave is very significant since this wave propagates large distances (much larger than L) along the grating before reaching resonantly large steady-state amplitudes. Therefore, scattered wave amplitudes can be noticeably reduced even by small dissipation. The reduction of the scattered wave amplitude results in the reduction of the amplitude of the re-scattered wave. Therefore, the re-scattered wave reaches the magnitude $|E_{00}|$ at larger distances from the front boundary, i.e. beyond the middle of the grating. As a result, the minimum of the overall incident wave amplitude $E_0(x)$ (i.e. the sum of amplitudes of the incident and re-scattered waves) moves to the right, closer to the rear grating boundary (Fig. 3a). This results in decreasing amplitude of the transmitted wave $E_{01} \equiv E_0(x)|_{x=L}$ (Fig. 4). When the dissipation is increased further, then the amplitude of the re-scattered wave at the rear boundary decreases faster than the amplitude of the incident wave $E_{00}\exp\{-\alpha_0 L/\cos(\theta_0)\}$. As a result, the amplitude E_{01}, after going through a minimum, must increase, because the incident wave will be less affected by the rapidly weakening re-scattered wave. This accounts for the minima of the transmitted wave amplitude within the range of e_2 from $\sim 10^{-6}$ to $\sim 10^{-4}$ in Fig. 4.

For narrow gratings (with $L < L_c$, where L_c is given by (8)) the minima of the transmitted wave amplitude E_{01} are far from 0 and only weakly depend on L. For example, the minimal values of $|E_{01}/E_{00}|$ for curves 1 and 2 in Fig. 4 are approximately equal to 0.42 and 0.34, respectively. At the same time, decreasing the grating width below the critical width results in a noticeable shift of the observed minima to the left, i.e. to smaller values of e_2 (compare curves 1 and 2 in Fig. 4). This is expected, because the resonance in narrower gratings is sharper and stronger, and therefore EAS must be more sensitive to weak dissipation.

If the grating width is close to, or larger than, L_c, then the situation changes. The minimum of the transmitted wave amplitude quickly becomes deeper with increasing L (see curves 3 and 4 in Fig. 4). It is very interesting that at $L = L_c$ the minimal value of E_{01} is equal to zero (see curve 4 in Fig. 4). If we increase the grating width further (beyond L_c), then the minimum of E_{01} increases (see curve 5 in Fig. 4), and then decreases back to approximately zero for grating widths that are significantly larger than the critical width (curve 6 in Fig. 4).

Figure 4 has been plotted for a particular grating amplitude $\varepsilon_1 = 5 \times 10^{-3}$. Nevertheless, the observed behaviour of the transmitted wave amplitude E_{01} is not restricted to this particular value of ε_1. It is typical for EAS in weakly dissipative gratings with different grating amplitudes. In particular, for a grating with an arbitrary amplitude (within the limits given by condition (3)), if $L = L_c$, it is possible to choose the imaginary part of the mean permittivity so that $E_{01} = 0$.

Figure 5 shows the dependences of relative transmitted wave amplitudes on e_2 for different values of ε_1. For each of the curves in this figure the grating width is equal to the critical width ($L = L_c$) determined by (8). It can be seen that the behaviour of the transmitted wave amplitudes as functions of dissipation is very similar for all grating amplitudes. The main difference between the presented curves is that the minimal (zero) values of E_{01} are achieved at different values of e_2 – the smaller the grating amplitude, the smaller the value of e_2 at which the zero amplitude E_{01} is achieved – Fig. 5. The minimal values of the transmitted wave amplitudes do not exactly reach zero in Fig. 5. This is because (8) gives only approximate values of L_c. For any grating amplitude, the grating width can be slightly adjusted further to obtain the exact zero of E_{01}.

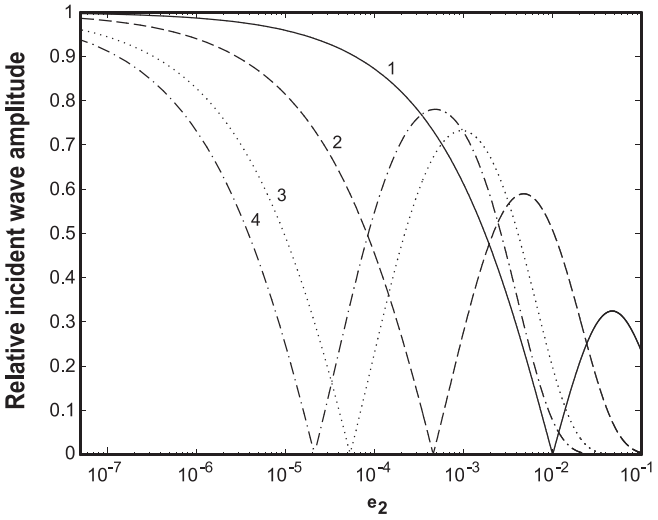

FIGURE 5 The dependences of the relative transmitted wave amplitudes $|E_{01}/E_{00}|$ at the rear boundary, $x = L$, on the imaginary part e_2 of the mean permittivity ε: (1) $|\varepsilon_1| = 5 \times 10^{-2}$, $L = L_c \approx 5.9\,\mu$m, (2) $|\varepsilon_1| = 5 \times 10^{-3}$, $L = L_c \approx 27.4\,\mu$m, (3) $|\varepsilon_1| = 1 \times 10^{-3}$, $L = L_c \approx 80.2\,\mu$m, (4) $|\varepsilon_1| = 5 \times 10^{-4}$, $L = L_c \approx 127.2\,\mu$m

Note that zero amplitude of E_{01} of the transmitted wave means that all energy of the incident wave (except for a small part of this energy that is lost due to direct dissipation of the incident wave within the distance $L/\cos\theta_0$) is transferred into the energy of the scattered wave and dissipates in the grating due to dissipation of the resonantly strong scattered wave.

Though (8) gives only approximate values of L_c [5, 6], it is amazingly accurate in the determination of the grating width at which the minimum of the amplitude E_{01} equals zero. In accordance with the derivation of (8), based on the consideration of re-scattering and diffractional divergence for the scattered wave [5, 6], one could expect that this equation must only give an order of magnitude for L_c. Nevertheless, numerical analysis shows that, for example, for bulk TE waves in gratings with $\varepsilon_1 = 5 \times 10^{-3}$, $e = 5$, $\theta_0 = \pi/4$, and λ (vacuum) $= 1$ mm, (8) gives $L_c \approx 27.4\,\mu$m (this corresponds to curve 4 in Fig. 4 and curve 2 in Fig. 5). This value is surprisingly close to the value $L \approx 27.7\,\mu$m for which the minimum of curve 2 in Fig. 5 would practically reach zero.

The same situation occurs for other values of the grating amplitude – see curves 1, 3, and 4 in Fig. 5 (for all these curves the grating width $L = L_c$ has been calculated using (8)). This is obviously not a mere coincidence. Equation (8) was derived on the basis of a clear understanding of physical processes

during scattering in the geometry of EAS [5, 6]. The critical grating width is an extremely important characteristic for all types of EAS without dissipation [5–7]. Therefore, it is not a surprise that the critical width also plays a significant role for EAS in weakly dissipative gratings. What is really surprising is that (8) appears to be that accurate in determining conditions for the zero amplitude of the transmitted wave. This once again demonstrates the correctness and the power of the developed new approach based on the allowance for the diffractional divergence of the scattered wave.

As has been demonstrated in [9, 10], the approximate and rigorous analyses of EAS in non-dissipative gratings with the parameters used for Figs. 2–5 give practically indistinguishable dependences of the scattered and incident wave amplitudes. The presence of dissipation results in decreasing scattered wave amplitudes, and the accuracy of the described approximate method improves even further (see also [7, 9]). Therefore, the curves presented in Figs. 2–5 can equally be regarded as approximate and rigorous (within the accuracy of $\sim 0.1\%$).

4 EAS of guided modes

As has been mentioned above, the developed approach and the obtained results are directly applicable for EAS of weakly dissipating optical modes guided by a slab with a periodically corrugated boundary. In this case, the plane of Fig. 1 is the slab interface that is periodically corrugated within the strip of width L (Fig. 1). A slab mode with the wave vector $\boldsymbol{k}_0$ is incident onto the grating region ($0 < x < L$) at an angle θ_0 (Fig. 1), and is scattered by the corrugation into another scattered guided mode (with the wave vector $\boldsymbol{k}_1$) of the same slab.

The parameters of such a structure can be selected so that Figs. 2–5 give the correct amplitudes of the incident and scattered slab modes. This can be done using an important general feature of EAS, which has been discussed in [10]. Namely, increasing (decreasing) the wavelength p times with the simultaneous increase (decrease) of the grating width p times leaves the amplitudes of the scattered and incident waves unchanged (though scaled to the different grating width). The same statement is also correct in the presence of dissipation. For example, EAS of bulk TE waves of $\lambda = 2\ \mu$m in a grating with $L = 160\ \mu$m is represented by exactly the same curves as in Figs. 2c and 3c, if we put $x/2$ on the horizontal axis instead of x (scaling to the two times larger grating width) and assume that all other structural parameters are the same as for Figs. 2c and 3c. Similarly, a p times increase (decrease) of the dielectric permittivity in the structure (including e_1, e_2, and the grating amplitude ε_1) with the simultaneous $\sqrt{p}$ times decrease (increase) of the grating width also leaves the wave amplitudes unchanged (though again scaled to the different grating width).

The same scaling procedure can be applied for EAS of guided slab modes in a corrugated slab. However, in this case, we have to consider effective dielectric permittivities determined for the incident and scattered slab modes. For example, consider a layered structure: substrate (dielectric permittivity is 4)–slab (permittivity is 5)–cladding (permittivity is 1) with the mean slab thickness $h = 0.6\ \mu$m (inside and outside the grating region). The corrugation of one of the surfaces of the slab is sinusoidal and restricted to the region $0 < x < L$ (Fig. 1):

$$h_\mathrm{s} = \begin{cases} h + \xi_\mathrm{g} \sin(x_0) & \text{if } 0 < x < L\,, \\ h & \text{otherwise,} \end{cases} \tag{9}$$

where h_s is the local slab thickness in the structure, the x_0 axis is normal to the grating fringes (Fig. 1), ξ_g is the corrugation amplitude, $\boldsymbol{k}_0$ and $\boldsymbol{k}_1$ in (4)–(6) are the real parts of the wave vectors of the incident and scattered slab modes, and α_0 and α_1 are the dissipation coefficients for the incident and scattered slab modes.

If the wavelength in vacuum is $\lambda = 1\ \mu$m, then the wave number of the TE zeroth mode (TE_0 mode) is $k_0 \approx 13.556 \times 10^4\ \mathrm{cm}^{-1}$, which corresponds to the effective dielectric permittivity of the structure $e_{1\,\mathrm{eff}} \equiv (k_0 c/\omega)^2 \approx 4.655$. Consider EAS of a TE_0 incident mode into a TE_0 scattered mode. Then, similarly to bulk waves in Sect. 3, $k_1 = k_0$ and $\alpha_1 = \alpha_0$. In this case, $e_{1\,\mathrm{eff}}$ is approximately 1.07 times less than the real part of the mean permittivity in the gratings considered for Figs. 2–5. Therefore, according to the scaling procedure (see above and [10]), the slab structure resulting in the same dependences such as, for example, in Figs. 2c and 3c must have the parameters: $L = 80(e_1/e_{1\,\mathrm{eff}})^{1/2} \approx 82.9\ \mu$m and

$$\alpha_0 = \alpha_1 \approx \frac{\omega e_{2\,\mathrm{eff}}}{2c\sqrt{e_{1\,\mathrm{eff}}}}\,, \tag{10}$$

where $e_{2\,\mathrm{eff}} = e_2 e_{1\,\mathrm{eff}}/e_1$, e_1 and e_2 take the values from the figure captions for Figs. 2c and 3c. The required corrugation amplitude must be obtained by means of the final adjusting of the resultant dependences to the curves in Figs. 2c and 3c. This is done by the analysis of solutions to (5) and (6) with Γ_1 and Γ_0 determined by the mode-matching theory [18, 22–27] (see also [4]). This analysis confirms that Figs. 2c and 3c correspond to EAS of TE_0 incident modes into TE_0 scattered modes in the considered structure if the corrugation amplitude $\xi_\mathrm{g} = 1.7 \times 10^{-6}$ cm, and we have $x(e_{1\,\mathrm{eff}}/e_1)^{1/2} \approx 0.97x$ instead of x on the horizontal axis.

In the same way, Figs. 2a,b and 3a,b describe EAS of TE_0 incident modes into TE_0 scattered modes in the structures with the same parameters but with grating widths $L = 10(e_1/e_{1\,\mathrm{eff}})^{1/2} \approx 10.3\ \mu$m and $L = 27.4(e_1/e_{1\,\mathrm{eff}})^{1/2} \approx 28.2\ \mu$m.

5 Physical analogies of EAS

The observed pattern of scattering in the geometry of EAS in the presence of weak dissipation makes it possible to draw analogies between EAS and other resonant wave effects, such as attenuated total reflection [12–14], resonant tunnelling of waves in layered structures [16, 17], Fabry–Pérot interferometry [15], resonant rotation of a mirror-reflected wave [18], etc. For example, in the case of ATR in the structure prism–vacuum gap–metal (i.e. in the geometry of Otto [12]) we have resonant generation of surface plasmons on a metal surface by means of a prism coupler. This occurs when the tangential (to the metal surface) component of the wave vector of the incident wave in the prism is equal to the wave vector of the surface wave at the metal surface (Snell's law for the incident and surface waves) [12, 14]. It is well

known that in the resonance, for a given gap width, the reflected wave amplitude decreases with increasing imaginary part of the metal permittivity, goes through a minimum (which is usually close to zero), and then increases back to about the amplitude of the incident wave. This is very similar to what is observed in Fig. 4 for EAS. This suggests that the reflected wave in ATR is analogous to the transmitted wave in EAS. Similarly, gap width in ATR is analogous to grating amplitude in EAS (increasing gap width is analogous to decreasing grating amplitude). The scattered and re-scattered waves in EAS are analogous to the surface and leaky waves in ATR, respectively. The resonance condition for ATR (i.e. Snell's law for the incident and surface waves) is analogous to the Bragg condition in EAS.

Similarly, if a bulk wave is resonantly transmitted through a Fabry–Pérot interferometer (a plate with semi-transparent mirrors [15]), then the resonantly strong wave between the mirrors is analogous to the scattered wave. Reflectivity of the mirrors is analogous to grating amplitude in EAS (increasing reflectivity is similar to decreasing grating amplitude). The resonant condition for the formation of a standing wave pattern between the mirrors is analogous to the Bragg condition in EAS. The reflected wave from the Fabry–Pérot interferometer is analogous to the transmitted wave in EAS; if the rear mirror of the interferometer is 100% reflective and the front mirror is still semi-transparent, then the dependence of the reflected wave amplitude on dissipation between the mirrors is very similar to that of the transmitted wave in Fig. 4. Finally, the leaky waves in the interferometer (e.g. the transmitted wave) are analogous to the re-scattered wave in EAS. Similar analogies can easily be drawn between EAS and other mentioned resonant wave effects in layered structures.

On the other hand, EAS has unique features that make it significantly different from other resonant optical effects. This is due to the complexity of EAS, involving two main physical phenomena – Bragg scattering and diffractional divergence of the scattered wave. For example, grating width has no analogies in ATR, Fabry–Pérot interferometry, etc. Therefore, numerous important features of EAS related to varying grating width do not have analogies with other resonant effects in optics. In particular, critical grating width and the related numerous effects are unique to EAS. Obviously, the field structure in the incident and scattered waves inside and outside the grating is also completely different from that for ATR.

6 Conclusion

In this paper the recently developed new method, based on allowance of the diffractional divergence of the scattered wave, has been employed for the analysis of EAS of weakly dissipating bulk and guided optical waves in oblique periodic gratings. A detailed theoretical investigation of the steady-state field structure in the incident and scattered waves inside and outside the grating was carried out for different dissipation coefficients. In particular, it was demonstrated that, being a strongly resonant effect, EAS is very sensitive to small dissipation of waves inside and outside the grating. A unique role of the critical grating width is demonstrated for EAS of weakly dissipating waves. As previously [5, 6], half of this width is equal to the distance that the scattered wave can be spread across the grating by means of the diffractional divergence, before being re-scattered by the grating.

The results of this paper are immediately applicable for the description of EAS of all types of waves, including bulk, surface, and guided electromagnetic and acoustic waves, in different types of periodic gratings. The only thing that should be altered in the coupled wave equations, when we change from one type of waves to another, are the numerical values of the coupling coefficients (that are determined in the conventional theories of Bragg scattering without dissipation [18–27] (see also [4])). Typical examples of EAS of modes guided by a slab with a corrugated interface have been considered.

It has been demonstrated that EAS in the presence of weak dissipation makes it possible to draw deep analogies between EAS and other resonant wave effects, such as attenuated total reflection, resonant tunnelling of waves in layered structures, Fabry–Pérot interferometry, resonant rotation of a mirror-reflected wave, etc. [12–15, 18]. On the other hand, it has also been shown that EAS has unique features that make it significantly different from other resonant optical effects. A physical explanation of the predicted effects has been presented.

REFERENCES

1 M.P. Bakhturin, L.A. Chernozatonskii, D.K. Gramotnev: Appl. Opt. **34**, 2692 (1995)
2 D.K. Gramotnev: Phys. Lett. A **200**, 184 (1995)
3 D.K. Gramotnev: J. Phys. D **30**, 2056 (1997)
4 D.K. Gramotnev: Opt. Lett. **22**, 1053 (1997)
5 D.K. Gramotnev, D.F.P. Pile: Phys. Lett. A **253**, 309 (1999)
6 D.K. Gramotnev, D.F.P. Pile: Opt. Quantum Electron. **32**, 1097 (2000)
7 D.K. Gramotnev: Opt. Quantum Electron. **33**, 253 (2001)
8 D.K. Gramotnev, D.F.P. Pile: J. Opt. A: Pure Appl. Opt. **3**, 103 (2001)
9 T.A. Nieminen, D.K. Gramotnev: Opt. Commun. **189**, 175 (2001)
10 D.K. Gramotnev, T.A. Nieminen, T.A. Hopper: J. Mod. Opt. **49**, 1567 (2002)
11 D.K. Gramotnev: In: Proc. Diffr. Opt. Micro-Opt. (DOMO-2000), Quebec, Canada (2000) p. 165
12 A. Otto: Z. Phys. **216**, 398 (1968)
13 E. Kretschmann: Z. Phys. **241**, 313 (1971)
14 H. Raether: *Surface Plasmons on Smooth and Rough Surfaces and on Gratings* (Springer, Berlin 1988)
15 M. Born, E. Wolf: *Principles of Optics* (Pergamon, Oxford 1975)
16 R. Dragila, B. Luther-Davies, S. Vukovic: Phys. Rev. Lett. **55**, 1117 (1985)
17 R.R. Ramazashvili: JETP Lett. **43**, 298 (1986)
18 M.P. Bakhturin, D.K. Gramotnev: Phys. Lett. A **162**, 485 (1992)
19 D.G. Hall: Opt. Lett. **15**, 619 (1990)
20 G.I. Stegeman, D. Saird, J.J. Burke, D.G. Hall: J. Opt. Soc. Am. **71**, 1497 (1981)
21 H. Kogelnik: Bell Syst. Tech. J. **48**, 2909 (1969)
22 L.A. Weller-Brophy, D.G. Hall: J. Lightwave Technol. **6**, 1069 (1988)
23 E. Popov, L. Mashev: Opt. Acta **32**, 265 (1985)
24 W. Biehlig, K. Hehl, U. Langbein, F. Leberer: Opt. Quantum Electron. **18**, 219 (1986)
25 W. Biehlig: Opt. Quantum Electron. **18**, 229 (1986)
26 H. Shigesawa, M. Tsuji: IEEE Trans. Microwave Theory Tech. **34**, 205 (1986)
27 P.P. Borsboom, H.J. Frankena: J. Opt Soc. A **12**, 1134 (1995)